Organic & Biomolecular Chemistry

ROYAL SOCIETY OF CHEMISTRY

PAPER

View Article Online
View Journal | View Issue

Cite this: *Org. Biomol. Chem.*, 2025, **23**, 7786

Amino-acid derived benzazaboroles: structure and function of a new chemotype

Cyril J. O'Brien,[a] Elisa Ospanow,[a] Karin Reznikov,[a] Ebrahim Soleimani,[a] Martin Lanteigne,[c] Carol A. Tanner,[d] Bradley A. Haltli,[b,c] Gary I. Dmitrienko,[d] Katherine N. Robertson [e] and David L. Jakeman *[a,f]

Received 9th June 2025,
Accepted 1st August 2025

DOI: 10.1039/d5ob00948k

rsc.li/obc

The synthesis, structural characterization, and functional properties of a series of benzazaboroles are presented. These molecules are analogues of clinically relevant benzoxaboroles and exhibit unique structural features due to a nitrogen–boron (N–B) dative bond in aqueous media. The compounds were synthesized using a reductive amination and characterized through NMR spectroscopy and X-ray crystallography. Their structures were found to be pH-dependent, transitioning between trigonal and tetrahedral boron configurations, whilst maintaining the benzazaborole five-membered ring. The benzazaboroles demonstrated selective binding to diols and saccharides, with binding affinities influenced by the length of the amino acid side chain. Fluorescence assays revealed that shorter-chain derivatives preferentially bound glucuronic and sialic acids, while longer chains favored fructose. Although antimicrobial activity was limited, antifungal effects were observed with MIC_{90} values of 1.2 mM against *Candida albicans*, and one compound showed inhibitory activity against KPC-2, a class A beta-lactamase. These findings suggest the potential for further development of benzazaboroles as selective saccharide sensors, enzyme inhibitors and antifungal agents. The study provides foundational insights into the aqueous behavior and properties of this underexplored class of organoboron-containing molecules.

Introduction

Boron-containing pharmaceuticals are emerging as important clinical medicines to treat human disease (Fig. 1).[1–4] Bortezomib was approved in 2004 for the treatment of multiple myeloma,[5] and followed by the 2015 approval of *ixazomib*, a second-generation *boron-based proteasome inhibitor*.[6] Tavaborole was approved in 2014 as a topical antifungal,[7] crisaborole was approved in 2016 as a topical eczema treatment[8] and vaborbactam was approved in 2024 as a beta-lactamase inhibitor to treat multidrug-resistant bacteria.[9] Other boron-containing molecules are in clinical trials for additional diseases.[10] The presence of the boron atom is pivotal to drug action.[11] The mild Lewis acidic property of the boronic acid facilitates the reversible formation of boronate complexes with alcohols or carboxylic acids under biological conditions,[12,13] accounting for the mechanism of action for these approved drugs. Molecules containing boron are also clinically used for boron neutron capture therapy to deliver radiation to various aggressive cancers.[14] In addition to advancing treatment of human disease, boron-containing molecules also offer unique opportunities in the fields of carbohydrate recognition,[15–18] and catalysis,[19–21] and as biomaterials.[22,23] Benzoxaboroles are relatively widely studied[10,22] and include tavaborole and crisaborole as clinically approved drugs. By contrast, Benzazaboroles[24,25] are less widely studied isosteric analogues of benzoxaboroles. Benzazaboroles (Scheme 1) include a substituent on the nitrogen atom that coordinates to the boron atom, providing additional

[a]*Department of Chemistry, Dalhousie University, Halifax, Nova Scotia, B3H 4J3, Canada*
[b]*Departments of Biomedical Sciences, University of Prince Edward Island, Charlottetown, Prince Edward Island, C1A 4P3, Canada*
[c]*Croda Canada Ltd, Charlottetown, Prince Edward Island, C1A 4P3, Canada*
[d]*Department of Chemistry, University of Waterloo, Waterloo, Ontario, N2L 3G1, Canada*
[e]*Department of Chemistry, Saint Mary's University, Halifax, Nova ScotiaB3H 3C3, Canada*
[f]*College of Pharmacy, Dalhousie University, Halifax, Nova Scotia B3H 4R2, Canada. E-mail: David.jakeman@dal.ca*

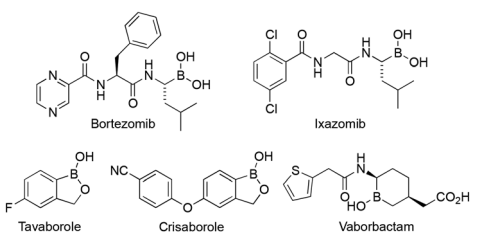

Fig. 1 Clinically-approved boron-containing drugs.

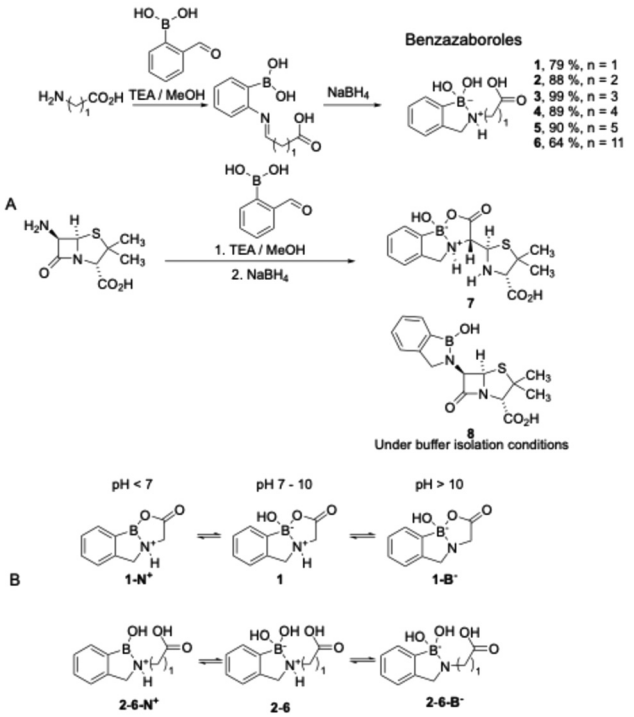

Scheme 1 (A) Preparation of benzazaboroles; (B) Proposed ionization states at differing pH based on multi-nuclear NMR titration data (Fig. 3).

opportunities to modify physicochemical properties and are distinct from "Wulff-type" dialkylamino analogues.[26]

Herein, we report the synthesis of a series of amino-acid derived benzazaboroles and provide insight into their structure and properties in aqueous solution, including the propensity for selective diol binding, antimicrobial and beta-lactamase activity.[27,28]

Results and discussion

Synthesis and characterization

The synthesis of the benzazaboroles **1–8** (Scheme 1A) utilized a one-pot two-step reductive amination procedure with the addition of amino acid to a slight excess of formylphenylboronic acid to furnish the imine adducts,[25] and subsequent treatment with sodium borohydride to reduce the imine to the secondary amine with concomitant cyclization into the benzazaborole **1–6**.[29] The amino acids chosen for the synthesis were readily accessible, having previously been used in the isolation of novel jadomycin natural products.[30,31] The purification of products from shorter chained amino acids (glycine, β-alanine, γ-aminobutyric acid) was achieved through trituration with tetrahydrofuran. The products from 5-aminovaleric acid and 6-aminohexanoic acid necessitated reversed-phase chromatography for purification, whilst the derivative from dodecanoic acid was purified through trituration. The preparative success with the linear amino acids led us to evaluate a structurally more complex substrate, 6-aminopenicillanic acid, a key building block that led to generations of penicillin antibiotics.[32] The resulting product would be a novel beta-lactam containing a benzazaborole. Given the discovery of potent beta-lactamase inhibitors incorporating boron,[33,34] the presence of a benzazaborole functionality in concert with the beta-lactam ring, could provide an additional site to interact with the active sites of metallo- or serine-beta-lactamases.[2,35,36] Thus, utilizing reaction conditions similar to those described above, 6-aminopenicillanic acid and formylphenylboronic acid were reacted together. It was evident that a new product had been produced, as observed by TLC, NMR spectra analysis, and mass spectrometry data of the reaction mixture. Upon utilizing the standard work-up conditions, a crystalline product was isolated. Subsequently, this material was recrystallized and subjected to single crystal X-ray diffraction analysis (Fig. 2, see SI). Analysis of the diffraction data identified a product that contained a benzazaborole functionality, however, the benzazaborole was complexed to a carboxylic acid, resulting from the hydrolysis of the beta-lactam ring. Inspection of the six chiral centres within the crystal structure of **7** indicated that C2, C3 and C4 possessed stereochemistry consistent with 6-aminopenicillanic acid, whilst both secondary amines were protonated in the crystal structure: the thiazolidine ring nitrogen having *S* configuration, and the benzazaborole ring nitrogen having *R* configuration. The final stereochemical centre was the boron atom, possessing *R* configuration. It is reasonable to propose that the chirality at the three heteroatoms (N1, N2, B1) is induced as a consequence of the chirality within the 6-aminopenicillanic acid upon crystallization. Preparation of the 6-aminopenicillanic derivative that maintained the beta-lactam ring was accomplished by changing the work-up conditions to include buffering with cold phosphate, and timely reversed-phase purification using phosphate buffer at pH 7. Sufficient quantities of the desired benzazaborole-6-aminopenicillanic acid derivative **8** were isolated enabling structural characterization by NMR spectroscopy, but remained hydrolytically labile, potentially due to the presence of the boron centre acting as a Lewis acid promotor, accelerating beta-lactam hydrolysis.

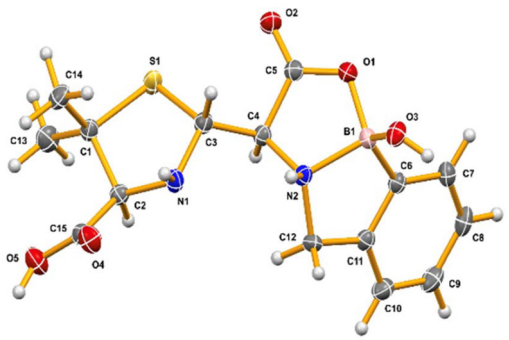

Fig. 2 Crystal structure of **7** (50% probability ellipsoids). Disorder and waters of hydration have been removed. Hydrogen atoms are included but not labelled. The tetrahedral boron atom (B1) with the dative N–B bond has *R* configuration. Both N1 and N2 have tetrahedral geometry, with *S* and *R* configuration, respectively.

Effects of pH on benzazaborole structure

Characterization data for the purified compounds were recorded in D_2O at pH 9.3. The ^{1}H signals were relatively broad, and limited splitting was observed (see SI). The ^{11}B NMR chemical shift is indicative of either a trigonal-sp^2 or tetrahedral-sp^3 environment at the boron nucleus.[37] The ^{11}B chemical shifts for **1–5** were between 8.4–6.1 ppm, which is consistent with the tetrahedral "ate" form of a boron atom. In order to probe the structure of **1–5** and **7** in aqueous solution and address the nature of the substituents around the boron atom, more detailed pH investigations of compounds **1–5** were conducted using ^{1}H and ^{11}B NMR (Fig. 3, see SI). There were significant changes to the spectra over the pH range 1–10, and these changes were reversible. At pH 9.3, the ^{1}H spectra were broad, consistent with the initial characterization data. By contrast, the pH 6.4 ^{1}H spectrum for **1**, showed two species with the appearance of AB NMR spin system between 4–4.5 ppm. By pH 4.4 the species observed at basic pH was completely absent. The species observed at low pH had substantially sharper lines and signals were split. Investigations by Contreras[38] into the preparation of boron heterocyclic complexes containing chiral nitrogen and boron atoms describe an AB NMR spin systems for the methylene protons between the nitrogen and carboxylic acid in DMSO, whilst Thiele and co-workers[39] observed similar NMR splitting with their related adducts in DMSO. Our data for **1**, is entirely consistent with Contreras and Thiele's observations in DMSO, where the methylene resonances were split. The ^{11}B NMR showed three discrete resonances over the pH range. At pH 10, a sharp peak at ~1 ppm was observed, likely a four-coordinate boron nucleus. At pH 9 the major resonance was at 6.5 ppm, albeit significantly broader, also likely a four-coordinate boron nucleus, and from pH 8 downwards, a signal at 19 ppm dominated, likely a three-coordinate boron nucleus. Similar trends for **2–5** were also observed in their ^{1}H and ^{11}B NMR. For **3–5** there was a more pronounced broadening of the signals around pH 6–7, indicative of slow-exchange on the NMR timescale. The ^{11}B NMR of **7** was recorded at pH 1.5 and 10.1. Only one sharp peak was observed at each pH, at ~19 ppm and ~6 ppm, respectively (see SI), whereas the spectrum of **7** at pH 8.1 consisted of both of these peaks. These two peaks were integrated and the Henderson–Hasselbach equation used to determine a p*K*a for the boron atom of 8.5 ± 0.4. These ^{11}B chemical shifts of **7** are consistent with those of **1–5**, and provide evidence of similar configuration around the boron atom for **1–5**.

We compared ^{13}C data for **1–4** and **7** (see SI) at pH 9.3. Analysis of the chemical shift for the carboxylic acids informed on whether the carboxylate cyclized onto the boron atom. Given the X-ray data indicated that compound **7** comprised of the carboxylate (formerly from the beta-lactam ring) coordinating to the boron centre, and the near identical chemical shift for the carboxylates in **7** and **1** (175.16 ppm for **7** and 175.62 ppm for **1**), suggest that **1** also exists as the cyclic boronate form at high pH. The chemical shifts for the carboxylates of **2–4** increased with increasing number of methylene substituents, with the carboxylate in **2** having a 5 ppm increase relative to the carboxylate in **1**, suggesting **2–4** exist in an acyclic form with respect to the carboxylic acid (Scheme 1B).

We hypothesize from interpretation of the ^{1}H, ^{11}B and ^{13}C NMR data, together with the crystal structure of **7**, that the species observed at acidic pH (<7) for **1** is a trigonal boron atom with the carboxylate coordinating to the boron, *i.e.* species **1-N$^+$** (Scheme 1B). As the pH increases, the next structural change occurs as a consequence of the pK_a at boron, converting from trigonal to tetrahedral, equilibrating to **1** exclusively by pH 9, and at pH > 10 deprotonation of the secondary amine is observed (**1-B$^-$**), resulting in the sharp ^{11}B peak at ~1 ppm. A similar series of equilibria exist for **7**. Whereas those compounds that do not have the ability to form a 5-membered ring with the carboxylate coordinating to boron *i.e.* **2–5**, (and by analogy **6**) exist at pH < 7 as trigonal benzazaborole species **2-N$^+$–5-N$^+$**, equilibrating to the boronate species **2–5** by pH 9, and at pH > 10 exist as the deprotonated secondary amine derivatives (**2-B$^-$–6-B$^-$**). The pH stability of our benzazaboroles contrasted with observed decomposition of a series of related benzazaboroles in water or protic solvents by ESI-MS,[40] although others were able to observe sufficient benzazaborole stability to demonstrate iodide binding.[41] There is conjecture in the literature as to whether N–B bonds exist to any significant extent in protic media.[13,42,43] The crystallization of **7** from an aqueous solution, and observation of the unequivocal N–B bond provides evidence that benzazaboroles comprise a dative N–B bond in aqueous media. Benzazaboroles that have previously been characterised crystallographically, where a clear dative N–B bond was observed were formed either as complexes,[44–49] or through crystallization from organic solvents.[41,50–52] The similar boron chemical shifts for **1–7**, across the pH 1–10 range (*vide infra*) suggest that **1–6** also comprise a N–B dative bond in aqueous media.

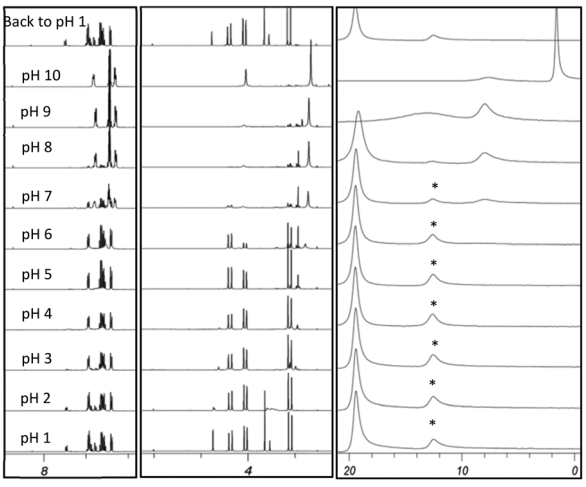

Fig. 3 ^{1}H and ^{11}B NMR data for **1** (full spectra available in SI). Left box: ^{1}H NMR aromatic region; middle box: ^{1}H NMR aliphatic region; right box ^{11}B NMR. *The peak at ~13 ppm in the ^{11}B NMR is boric acid.

Diol binding affinities for benzazaboroles

It is widely known that boronic acids and related boron-containing species bind 1,2-diols, and this phenomenon has resulted in the development of many synthetic receptors for glucose or other saccharides.[43,53–56] Quantitation of the affinity between boronic acids and diols is readily accomplished using the UV-vis or fluorescence method developed by Wang and Springsteen,[27,28] with a detailed mechanistic analysis by Benkovic.[57] The method relies upon the change in UV-absorbance, or turn-on fluorescence, as the alizarin red S (ARS) catechol forms a complex with a boronic acid (Scheme 2A). The affinity of benzazaboroles for ARS and other diols has not been described previously. Using this approach (Scheme 2B), the benzazaboroles were titrated into ARS and the resulting fluorescence data fitted to a 1 : 1 binding isotherm to quantify the affinity (Table 1, see SI). Data fitting was accomplished using Thordarson's[58,59] approaches, as previously described,[60] or adapting an Excel template for enzyme kinetics[61] to include the 1 : 1 binding isotherm.[62] None of the benzazaboroles bound to ARS with comparable affinity to phenylboronic acid, with **1** being the most potent, with a K_a 1/3rd that of phenylboronic acid. It is reasonable to propose that the presence of slow exchange between the equilibrium forms of **1–5** (as observed in the NMR spectra at pH 7–8) effects the strength of diol binding. There was a decrease in affinity as the chain length of the amino acid increased, and **5** bound with a K_a of 39. A boronic acid contains two hydroxyl substituents and the boron Lewis centre to accommodate the ARS catechol. By contrast, the benzazaboroles **1–5** contain intramolecular hydroxyl, amino and carboxylate substituents potentially interacting with boron. Thus, there are fewer coordination sites to readily accommodate the intermolecular catechol functionality. Nevertheless, given the fluorescence and UV-visible spectrum changes upon titration of ARS with the benzazaboroles **1–5**, it is reasonable to propose the formation of a complex as outlined in Scheme 2B. In an effort to provide more detailed structural information, we implemented the recently described $^{1}H–^{11}B$ HMBC NMR experiment[63] in an attempt to probe structures and complexes herein, without success.

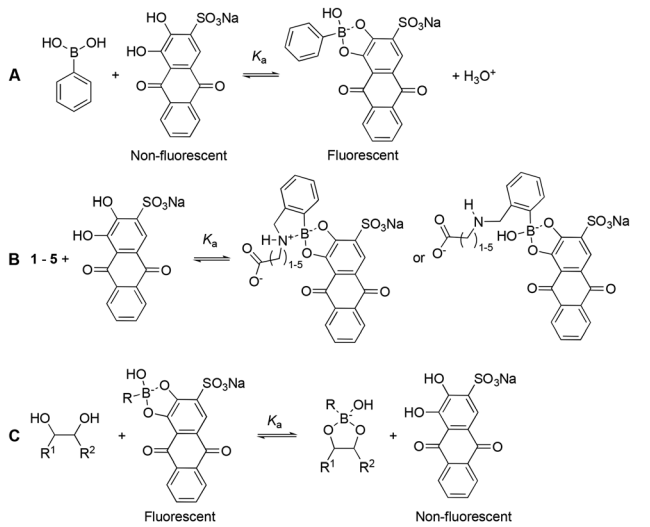

Scheme 2 Diol binding schemes. A. Phenylboronic acid and alizarin red S complex; B. representative benzazaborole and alizarin red S complexes; C. three-component saccharide binding.

Table 1 Binding affinities (K_a) measured for benzazaboroles binding to alizarin red S

Compound	K_a (M^{-1})[a]
Phenylboronic acid	1553 ± 1
1	387 ± 1
2	296 ± 0.3
3	114 ± 2
4	88 ± 0.2
5	39 ± 3

[a] HEPES (0.1 M), pH 7.4. Errors represent mean ± standard deviation.

The fluorescent three-component assay developed by Wang and Springsteen (Scheme 2C)[27] was used to measure relative affinities to diols generally through a competition experiment, where the fluorescent complex between boronic acid and ARS is titrated with a specific diol to determine the relative affinity. Given that the formation of fluorescent complexes with the benzazaboroles and ARS was readily accomplished, the affinity for ten saccharides (fructose, glucuronic acid, glucose, xylose, sialic acid, mannose, galactose, rhamnose, sucrose and glucosamine) was investigated. Thus, complexes of ARS-benzazaborole were formed and titrated with the saccharides (Table 2, see SI). Phenylboronic acid was included as a control, and had greatest affinity for fructose and sialic acid. Often fructose is a potent binder for boronic acid receptors. By contrast, benzazaboroles **1** and **2** both had greatest affinity for glucuronic acid and sialic acid, whereas **3–5** had greatest affinity for fructose or glucuronic acid. Interestingly, several of the sugars, including rhamnose, sucrose and glucosamine, showed no detectable affinity in this assay, particularly when considering that rhamnose contains a *cis*-diol that is often considered important for boronic acid binding. The data demonstrate that selectivity between saccharides is feasible. It is likely that in the future, developing boron-containing saccharide binding congeners where the ionization of the boronic acid does not result in slow-exchange processes in aqueous media at the pH where the diol binding experiments are conducted, will result in enhanced potency.

Antimicrobial activity of benzazaboroles

A panel of representative Gram-positive, Gram-negative and fungal organisms, including methicillin-resistant *Staphylococcus aureus* (MRSA), *Enterococcus faecalis*, *Staphylococcus warneri*, *Pseudomonas aeruginosa*, *Proteus vulgaris*, and *Candida albicans* were screened for growth inhibition by **1–3** (see SI). The dose–response data indicated that none of the bacterial strains experienced more than 25% growth inhibition at 1 mM. *C. albicans* was significantly more susceptible, with growth inhibition of 50% at 0.25–0.5 mM for

Table 2 Binding affinities (K_a) measured for interactions between benzazaboroles and saccharides using the 3-component ARS assay

	K_a[a]									
CPD	Fructose (M^{-1})	Glucuronic acid (M^{-1})	Glucose (M^{-1})	Xylose (M^{-1})	Sialic acid (M^{-1})	Mannose (M^{-1})	Galactose (M^{-1})	Rhamnose (M^{-1})	Sucrose (M^{-1})	Glucosamine (M^{-1})
PBA	117 ± 1	27 ± 5	4 ± 1	5 ± 5	54 ± 28	9 ± 1	5 ± 0.4	n.b	n.b	n.b
1	31 ± 6	231 ± 1	n.b.	8 ± 4	84 ± 13	27 ± 5	5 ± 2	n.b	n.b	n.b
2	29 ± 2	134 ± 1	8 ± 1	8 ± 6	85 ± 4	n.b.	n.b.	n.b	n.b	n.b
3	30 ± 2	64 ± 1	2 ± 1	10 ± 1	7 ± 0.2	n.b.	3 ± 2	n.b	n.b	n.b
4	41 ± 2	39 ± 1	n.b.	4 ± 3	10 ± 6	6 ± 1	n.b.	n.b	n.b	n.b
5	72 ± 2	59 ± 2	3 ± 1	7 ± 2	n.b.	2 ± 2	3 ± 2	n.b	n.b	n.b

n.b. = no significant binding. [a] HEPES (0.1 M), pH 7.4. Errors represent mean ± standard deviation.

all three compounds tested. Calculated MIC_{90} values for *C. albicans* were determined to be ~1.2 mM. This activity against the fungal species is consistent with the role of benzoxaborole, tavaborole, as an approved antifungal agent, given the structural similarities. Structural optimization may lead to benzazaboroles with improved activity.

Beta-lactamase inhibition of benzazaboroles

The role of the benzazaboroles as potential beta-lactamase inhibitors was explored with **1** and **2**. The compounds were evaluated against a panel of seven recombinant serine and metallo beta-lactamases, including enzymes from classes A–D.[64] Compounds were preincubated with the enzyme (10 min) prior to initiating the enzymatic reaction with addition of nitrocefin as substrate. Three different inhibitor concentrations were screened, namely 100, 10 and 1 μM. Only KPC-2, a class A carbapenemase, was susceptible, with 60% and 50% activity at 100 μM for **1** and **2**, respectively. The activity increased to 95% and 86% at the 10 μM concentration. This indicates that benzazaboroles have activity against KPC-2, a serine beta-lactamase, and suggests that structural optimization may lead to more potent specific inhibitors.

Conclusions

A series of novel benzazaboroles were synthesized and structurally characterized. There is a reversible pH dependence on the structure of the benzazaboroles, primarily relating to the conversion of the trigonal boron to tetrahedral boron around neutral pH, whilst at basic pH (>10) deprotonation of the secondary amine is proposed. Evidence for the presence of a dative N–B bond was obtained through a crystal structure of the benzazaborole isolated from the derivatization and reaction of 6-aminopenicillanic acid. This adduct also provided structural insight into the intramolecular cyclization of the carboxylate onto the boron atom. This cyclization was not observed for those derivatives with multiple methylene functionality between the amino and carboxy functionality. The benzazaboroles were investigated as diol binding agents using fluorescence assays. As the chain length increased between the amino and carboxy functionality, the affinity decreased for alizarin red S. As of now, it is unclear why the binding decreases with increasing chain length, further investigation into that matter is needed. Each of the benzazaboroles was investigated for saccharide binding and preferences to different sugars were observed. The shorter chained benzazaboroles preferentially bound glucuronic acid or sialic acid, whilst the longer chained analogues bound fructose or glucuronic acid. These investigations provide the first insights into benzazaborole-diol binding recognition and the structural characteristics of these water-soluble saccharide sensors. Their antifungal activity, and their activity against KPC-2, a class A carbapenemase, provides opportunities for structure–activity improvement to deliver more potent benzazaboroles.

Author contributions

Conceptualisation: D. L. J. Funding acquisition D. L. J., G. I. D. Investigation C. J. O, E. O., K. R., E. O., K. N. R., M. L., C. A. T. Project administration: D. L. J. Supervision: B. A. H., G. I. D., D. L. J. Writing – original drafts, review and editing: C. J. O., E. O., K. R., C. A. T., K. N. R., B. A. H. and D. L. J.

Conflicts of interest

There are no conflicts to declare.

Data availability

The data supporting this article have been included as part of the SI.

Supplementary information is available. Including compound characterization, spectroscopic, biochemical, and antimicrobial data. See DOI: **https://doi.org/10.1039/d5ob00948k**.

CCDC 2452130 contains the supplementary crystallographic data for this paper.[65]

Acknowledgements

This work was supported, in part, by funding from NSERC and CIHR.

References

1 R. J. Grams, W. L. Santos, I. R. Scorei, A. Abad-García, C. A. Rosenblum, A. Bita, H. Cerecetto, C. Viñas and M. A. Soriano-Ursúa, *Chem. Rev.*, 2024, **124**, 2441–2511.
2 K. Messner, B. Vuong and G. K. Tranmer, *Pharmaceuticals*, 2022, **15**, 264.
3 L. Ji and H. Zhou, *Tetrahedron Lett.*, 2021, **82**, 153411.
4 C. T. Liu, J. W. Tomsho and S. J. Benkovic, *Bioorg. Med. Chem.*, 2014, **22**, 4462–4473.
5 S. Touchet, F. Carreaux, B. Carboni, A. Bouillon and J.-L. Boucher, *Chem. Soc. Rev.*, 2011, **40**, 3895–3914.
6 B. A. Teicher and J. E. Tomaszewski, *Biochem. Pharmacol.*, 2015, **96**, 1–9.
7 S. J. Baker, Y.-K. Zhang, T. Akama, A. Lau, H. Zhou, V. Hernandez, W. Mao, M. R. K. Alley, V. Sanders and J. J. Plattner, *J. Med. Chem.*, 2006, **49**, 4447–4450.
8 T. Akama, S. J. Baker, Y.-K. Zhang, V. Hernandez, H. Zhou, V. Sanders, Y. Freund, R. Kimura, K. R. Maples and J. J. Plattner, *Bioorg. Med. Chem. Lett.*, 2009, **19**, 2129–2132.
9 S. J. Hecker, K. R. Reddy, M. Totrov, G. C. Hirst, O. Lomovskaya, D. C. Griffith, P. King, R. Tsivkovski, D. Sun, M. Sabet, Z. Tarazi, M. C. Clifton, K. Atkins, A. Raymond, K. T. Potts, J. Abendroth, S. H. Boyer, J. S. Loutit, E. E. Morgan, S. Durso and M. N. Dudley, *J. Med. Chem.*, 2015, **58**, 3682–3692.
10 M. Z. H. Kazmi, O. M. Schneider and D. G. Hall, *J. Med. Chem.*, 2023, **66**, 13768–13787.
11 S. Song, P. Gao, L. Sun, D. Kang, J. Kongsted, V. Poongavanam, P. Zhan and X. Liu, *Acta Pharm. Sin. B*, 2021, **11**, 3035–3059.
12 S. D. Bull, M. G. Davidson, J. M. H. van den Elsen, J. S. Fossey, A. T. A. Jenkins, Y.-B. Jiang, Y. Kubo, F. Marken, K. Sakurai, J. Zhao and T. D. James, *Acc. Chem. Res.*, 2013, **46**, 312–326.
13 X. Sun, B. M. Chapin, P. Metola, B. Collins, B. Wang, T. D. James and E. V. Anslyn, *Nat. Chem.*, 2019, **11**, 768–778.
14 H. Xu, J. Liu, R. Li, J. Lin, L. Gui, Y. Wang, Z. Jin, W. Xia, Y. Liu, S. Cheng and Z. Yuan, *Coord. Chem. Rev.*, 2024, **511**, 215795.
15 W. L. A. Brooks, C. C. Deng and B. S. Sumerlin, *ACS Omega*, 2018, **3**, 17863–17870.
16 C. A. McClary and M. S. Taylor, *Carbohydr. Res.*, 2013, **381**, 112–122.
17 G. T. Williams, J. L. Kedge and J. S. Fossey, *ACS Sens.*, 2021, **6**, 1508–1528.
18 X. Zhang, G. Liu, Z. Ning and G. Xing, *Carbohydr. Res.*, 2017, **452**, 129–148.
19 D. G. Hall, *Chem. Soc. Rev.*, 2019, **48**, 3475–3496.
20 S. P. Desai, G. Yatzoglou, J. A. Turner and M. S. Taylor, *J. Am. Chem. Soc.*, 2024, **146**, 4973–4984.
21 M. S. Taylor, *Acc. Chem. Res.*, 2015, **48**, 295–305.
22 A. Adamczyk-Woźniak, K. M. Borys and A. Sporzyński, *Chem. Rev.*, 2015, **115**, 5224–5247.
23 W. L. A. Brooks and B. S. Sumerlin, *Chem. Rev.*, 2016, **116**, 1375–1397.
24 S. Kuwano, Y. Hosaka and T. Arai, *Chem. – Eur. J.*, 2019, **25**, 12920–12923.
25 S. Kuwano, Y. Hosaka and T. Arai, *Org. Biomol. Chem.*, 2019, **17**, 4475–4482.
26 M. Dowlut and D. G. Hall, *J. Am. Chem. Soc.*, 2006, **128**, 4226–4227.
27 G. Springsteen and B. Wang, *Chem. Commun.*, 2001, 1608–1609.
28 G. Springsteen and B. Wang, *Tetrahedron*, 2002, **58**, 5291–5300.
29 A. Adamczyk-Woźniak, M. K. Cabaj, P. M. Dominiak, P. Gajowiec, B. Gierczyk, J. Lipok, Ł. Popenda, G. Schroeder, E. Tomecka, P. Urbański, D. Wieczorek and A. Sporzyński, *Bioorg. Chem.*, 2015, **60**, 130–135.
30 C. F. Martinez-Farina and D. L. Jakeman, *Chem. Commun.*, 2015, **51**, 14617–14619.
31 J. M. MacLeod, S. M. Forget and D. L. Jakeman, *Can. J. Chem.*, 2018, **96**, 495–501.
32 G. N. Rolinson and A. M. Geddes, *Int. J. Antimicrob. Agents*, 2007, **29**, 3–8.
33 A. Parkova, A. Lucic, A. Krajnc, J. Brem, K. Calvopiña, G. W. Langley, M. A. McDonough, P. Trapencieris and C. J. Schofield, *ACS Infect. Dis.*, 2020, **6**, 1398–1404.
34 H. Newman, A. Krajnc, D. Bellini, C. J. Eyermann, G. A. Boyle, N. G. Paterson, K. E. McAuley, R. Lesniak, M. Gangar, F. von Delft, J. Brem, K. Chibale, C. J. Schofield and C. G. Dowson, *J. Med. Chem.*, 2021, **64**, 11379–11394.
35 C. L. Tooke, P. Hinchliffe, E. C. Bragginton, C. K. Colenso, V. H. A. Hirvonen, Y. Takebayashi and J. Spencer, *J. Mol. Biol.*, 2019, **431**, 3472–3500.
36 A. Krajnc, P. A. Lang, T. D. Panduwawala, J. Brem and C. J. Schofield, *Curr. Opin. Chem. Biol.*, 2019, **50**, 101–110.
37 S. A. Valenzuela, J. R. Howard, H. M. Park, S. Darbha and E. V. Anslyn, *J. Org. Chem.*, 2022, **87**, 15071–15076.
38 T. Mancilla and R. Contreras, *J. Organomet. Chem.*, 1987, **321**, 191–198.
39 N. A. Thiele, K. A. Abboud and K. B. Sloan, *Eur. J. Med. Chem.*, 2016, **118**, 193–207.
40 A. Rydzewska, K. Ślepokura, T. Lis, P. Kafarski and P. Młynarz, *Tetrahedron Lett.*, 2009, **50**, 132–134.
41 R. Zhang, Y.-D. Zhang, L.-X. Wang, C.-H. Ge, Z.-Y. Ma, J.-P. Miao and X.-D. Zhang, *Inorg. Chem. Commun.*, 2016, **74**, 52–57.
42 L. Zhu, S. H. Shabbir, M. Gray, V. M. Lynch, S. Sorey and E. V. Anslyn, *J. Am. Chem. Soc.*, 2006, **128**, 1222–1232.
43 J. A. Peters, *Coord. Chem. Rev.*, 2014, **268**, 1–22.
44 R. M. R. M. Lopes, A. E. Ventura, L. C. Silva, H. Faustino and P. M. P. Gois, *Chem. – Eur. J.*, 2018, **24**, 12495–12499.
45 K. Li, M. A. Kelly and J. Gao, *Org. Biomol. Chem.*, 2019, **17**, 5908–5912.
46 K. Li, C. Weidman and J. Gao, *Org. Lett.*, 2018, **20**, 20–23.
47 R. M. Reja, W. Wang, Y. Lyu, F. Haeffner and J. Gao, *J. Am. Chem. Soc.*, 2022, **144**, 1152–1157.
48 H. Faustino, M. J. S. A. Silva, L. F. Veiros, G. J. L. Bernardes and P. M. P. Gois, *Chem. Sci.*, 2016, **7**, 5052–5058.
49 A. Bandyopadhyay, S. Cambray and J. Gao, *Chem. Sci.*, 2016, **7**, 4589–4593.

50 T. Kliś and J. Serwatowski, *Tetrahedron Lett.*, 2007, **48**, 5223–5225.
51 M. Saito, K. Matsumoto, M. Fujita and M. Minoura, *Heteroat. Chem.*, 2014, **25**, 354–360.
52 J. Krajewska, K. Nowicki, K. Durka, P. H. Marek-Urban, P. Wińska, T. Stępniewski, K. Woźniak, A. E. Laudy and S. Luliński, *RSC Adv.*, 2022, **12**, 23099–23117.
53 G. F. Whyte, R. Vilar and R. Woscholski, *J. Chem. Biol.*, 2013, **6**, 161–174.
54 H. Cao and M. D. Heagy, *J. Fluoresc.*, 2004, **14**, 569–584.
55 M. G. Chudzinski, Y. Chi and M. S. Taylor, *Aust. J. Chem.*, 2011, **64**, 1466–1469.
56 A. M. Comiskey and E. V. Anslyn, *J. Org. Chem.*, 2025, **90**(22), 7161–7167.
57 J. W. Tomsho and S. J. Benkovic, *J. Org. Chem.*, 2012, **77**, 2098–2106.
58 P. Thordarson, *Chem. Soc. Rev.*, 2011, **40**, 1305–1323.
59 D. B. Hibbert and P. Thordarson, *Chem. Commun.*, 2016, **52**, 12792–12805.
60 A. Alkaş, J. M. Kofsky, E. C. Sullivan, D. Nebel, K. N. Robertson, C. J. Capicciotti, D. L. Jakeman, E. R. Johnson and A. Thompson, *Org. Biomol. Chem.*, 2024, **22**, 7448–7459.
61 A. Hernández and M. T. Ruiz, *Bioinformatics*, 1998, **14**, 227–228.
62 C. D. Douglas, L. Grandinetti, N. M. Easton, O. P. Kuehm, J. A. Hayden, M. C. Hamilton, M. St. Maurice and S. L. Bearne, *Biochemistry*, 2021, **60**, 2508–2518.
63 D. Kanyan, M. Horacek-Glading, M. J. Wildervanck, T. Söhnel, D. C. Ware and P. J. Brothers, *Org. Chem. Front.*, 2022, **9**, 720–730.
64 P. Hinchliffe, C. A. Tanner, A. P. Krismanich, G. Labbé, V. J. Goodfellow, L. Marrone, A. Y. Desoky, K. Calvopiña, E. E. Whittle, F. Zeng, M. B. Avison, N. C. Bols, S. Siemann, J. Spencer and G. I. Dmitrienko, *Biochemistry*, 2018, **57**, 1880–1892.
65 CCDC 2452130: Experimental Crystal Structure Determination, DOI: **10.5517/ccdc.csd.cc2n9mzl**.